Raindrop size distribution in warm rain as measured in Hawaii

By MIYUKI FUJIWARA, *Meteorological Research Institute, Tokyo, Japan*

(Manuscript received February 13, 1967)

ABSTRACT

On the eastern slope of the Island of Hawaii, raindrop size distributions were sampled simultaneously at 5 stations. From the data analyses, it was established that each sequence of data from one station represents the distribution of drops at various development stages. Then the representative data were inspected under the light of the author's previous paper (1965*b*) which concerns the classification for 4 processes, (1) coalescence between precipitable drops, (2) mixing of different groups, (3) accretion of cloud water, and (4) sorting of drops. The results show that most of the cases during the project have small values of A and b, where these parameters are defined by the radar reflectivity (Z) equation,

$$Z = AR^b, \quad R = \text{rainfall rate}.$$

This indicates that the mean diameters are smaller but that numbers are greater compared with continental showers. The analyses imply that the initial concentration of precipitable drops is very effective in determining the rainfall rates, especially in orographic rains.

1. Introduction

A great number of raindrop measurements have been made in Hawaii by Blanchard (1953), and Blanchard & Spencer (1957). The analysis of the drop size characteristics has been given in conjunction with data on sea salt nuclei by Woodcock & Blanchard (1955).

The author has studied the variation of the raindrop size distributions between storms (1965*a*) and their significant changes with precipitation mechanism (1965*b*). In the present project, it was intended to apply the conclusions obtained in these papers to the study of the mechanisms responsible for Hawaiian rainfall.

2. Observations

Five filter-paper raindrop recorders were placed along the saddle road at intervals of about 2 km. These stations are called E, B, C, D, A, beginning with that at the lowest elevation. (See Fig. 1 and Table 1.) Station B is the so called 9-mile site. One roll of filter paper is 12 cm wide, 270 m long and 0.1 mm thick. It is driven at approximately 1.5 cm/sec and lasts for about 5 hours. A rotating shutter was mounted above the opening of the device in order to reduce the sampling volume by a ratio 1/8 and to avoid the overlaping of flecks in the case of a heavy rain.

All 5 instruments were operated by one switch at the 9-mile base through a power line. Time marks were printed on the filter paper. The shutter is closed whenever the motor stops in order to prevent the recording paper from being damaged.

3. Observed Z–R characteristics

Since the radar reflectivety of the raindrops is defined as

$$Z = \Sigma D^6 \qquad (1)$$

a relationship between Z (mm^6/m^3) and the rainfall intensity R (mm/hr) is a characteristic of the raindrop size distribution. A and b are determined empirically from the drop size data and using the equation

$$Z = AR^b. \qquad (2)$$

Many empirical values for A and b have been published since radar was first used in meteorology. After L. Battan (1956), A ranges from 17 to 600, whereas b ranges from 1.24 to 2.87. Since the values range widely, an understanding of the variation is very important not only for

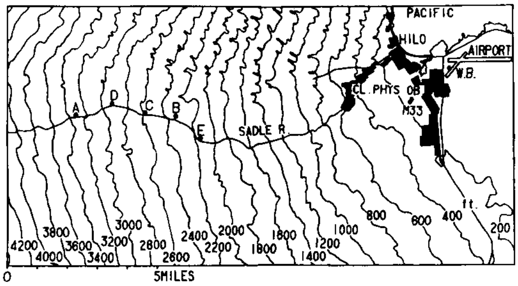

Fig. 1. Topography around the raindrop stations. Five raindrop Stations, A, D, C, B, and E are shown along the sadle road of the eastern slope of the Island of Hawaii. The airport and the radar site are also illustrated.

rainfall measurement but also in interpreting echoes. The values for Hawaiian rains are at the extreme of the range according to Blanchard (1953).

In Fig. 2, Blanchard's data (after Blanchard, 1953) are plotted with the author's which are

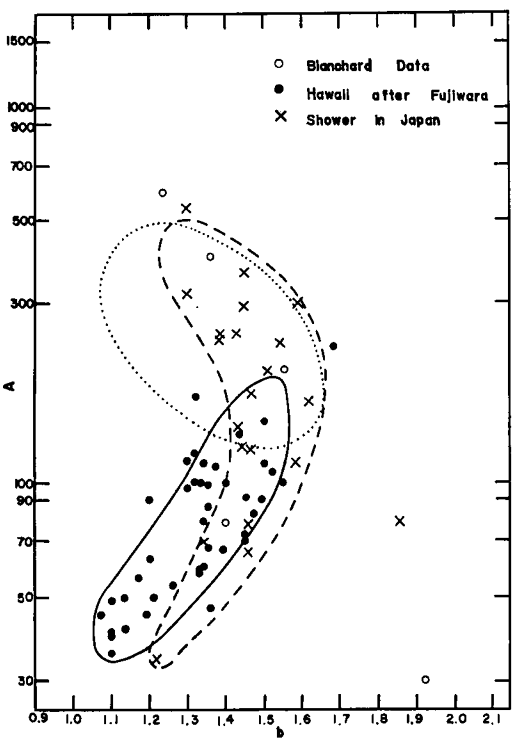

Fig. 2. A, b values (for the relationship $Z = AR^b$) observed in showers. The dotted region is after Fujiwara (1965*a*), which is determined with more continental data. Blanchard data is after Blanchard (1953).

Table 1

Station	Elevation from Sea level (m)
A	1030
D	888
C	798
B	715
E	651

Table 2. *$Z-R$ relationships calculated for every storm and station*

Obs.	St.	A	b	Remarks
28 July, 1701–1812	A	45	1.07	*A, b are* defined by $Z = AR^b$
	D	67	1.35	
	C	60	1.34	
	B	113	1.34	
	E	80	1.34	
	Mean	73	1.29	
31 July, 1647–1818	A	54	1.26	
	D	59	1.33	
	C	100	1.55	
	B	Not plotted		
	E	No data		
	Mean	71	1.38	
16 Aug., 1613–1625	A	(84)	1.47	Parentheses mean the value is uncertain.
	D	No rain		
	C	(114)	1.30	
	B	230	1.68	
	E	99	1.35	
	Mean	132	1.45	
18 Aug., 1826–1907	A	(58)	1.33	
	D	(66)	1.39	
	C	100	1.40	
	B	100	1.33	
	E	80	1.34	
	Mean	81	1.36	
21 Aug., 1620–1657	A	73	1.45	
	D	(49)	1.10	
	C	63	1.20	
	B	91	1.45	
	E	112	1.50	
	Mean	80	1.34	
23 Aug., 1124–1147	A	47	1.36	
	D	No data		
	C	47	1.19	
	B	41	1.15	
	E	39	1.10	
	Mean	43	1.20	
23 Aug., 1343–1401	A	35	1.10	
	D	50	1.21	
	C	50	1.13	
	B	(57)	1.17	
	E	(40)	1.10	
	Mean	46	1.14	

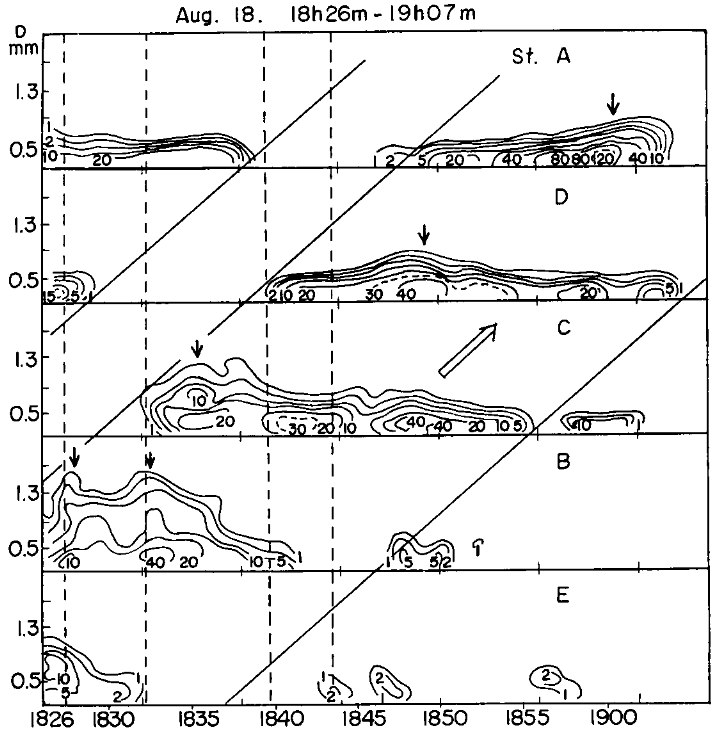

Fig. 3. N_D contour section with time on 18th August. Five small arrows show the peak concentrations. Other interpretation are given in Section 5.

also given in Table 2. Data were classified according to stations and storms before A and b were calculated. For comparison, the data of showers taken in Japan, where sometimes in Summer the prevailing air mass is maritime tropical, were plotted with symbols ×. The region encircled by dots contains the values for continental sources. The parameters for the weak Hawaiian showers are enclosed within an extreme region which extends down to $A = 35$ and $b = 1.1$. One characteristic of this distribution is that A increase with the exponent b, for which a brief explanation will be given in Sec. 11.

4. N_D contour sections

Generally speaking, large raindrops are generated in thick and heavy clouds either by accretion of cloud water droplets or by coalescence between raindrops. Illustrations of raindrop size distributions measured at the 5 stations are given in Figs. 3 and 4. The vertical axis shows the drop diameters in mm. The horizontal axis represents the sample number which may be interpreted as time. The isopleths show the concentrations of drops in the size intervals 0.2 mm per cubic meters. The period in which the outer contour reaches toward larger drop sizes suggests a thicker or denser cloud, probably due to increased convection. The peak around 1830 (sample 91) in Fig. 3 is in accordance with the convective part of the rain as revealed by a doppler radar observation given by Rogers & Jiusto (1966). The biggest drop size was 1.7 mm in diameter. At stations A and D, the drops were smaller than 1.0 mm and the size distribution was stationary, implying that the cloud was stratified.

5. Interpretation of N_D contour section by radar

As a part of the joint program, one M-33 3-cm radar was operated at the Hilo campus (See paper by Illinois group). Fig. 5 shows a rainband of the shower moving from northeast to southwest

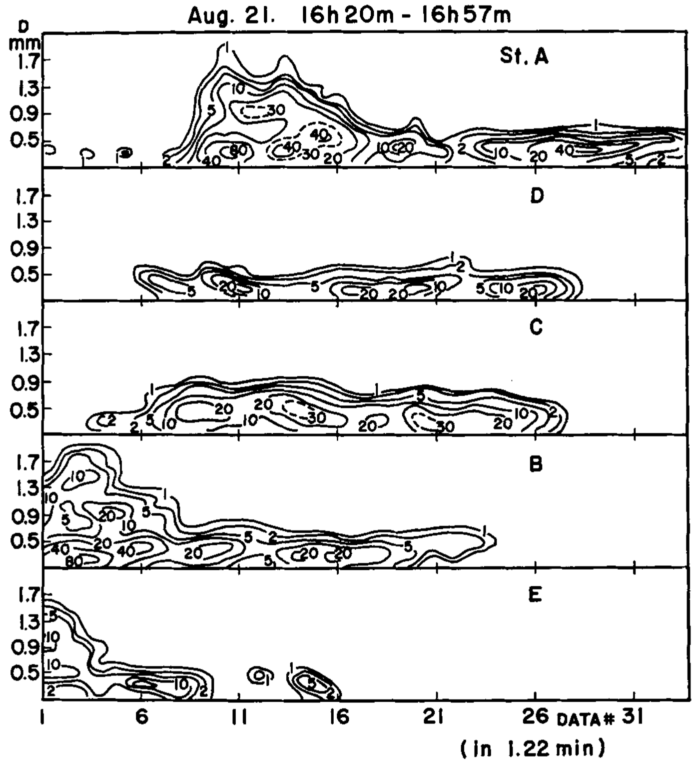

Fig. 4. N_D contour section with time on 21st August. Convective part is heading at Stations A, B, and E.

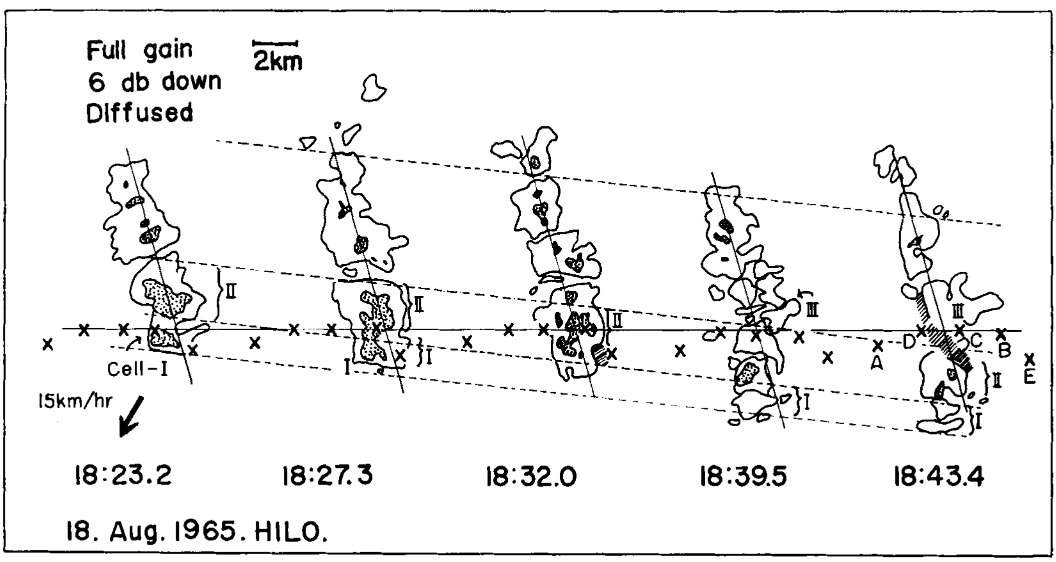

Fig. 5. The PPI echoes observed by M33, 3-cm radar, at the Cloud Physical Observatory, Hilo campus. The contours were made from the photographs according to favour of Mr. G. Stout, Illinois Water Survey. Interpretation is given in Section 5.

with the speed about 15 km/hr past the 5 raindrop stations, shown by ×. The axis of the band was tilted slightly to the west of north. The echo had started to become diffuse a few miles east of the 9-mile site, and evidently continued to spread out and to weaken during the period from 18:23.2 to 18:43.4.

The three cells I, II, and III, passed the stations during the 50 minute period from 18:20 to 19:10. Although there are some differences of intensity between cells, roughly speaking, the difference was more remarkable between observed times. The times corresponding to the echoes shown in Fig. 5 are shown in Fig. 3 by four broken lines. The raindrop data taken in the rainband are those illustrated between two slant lines in Fig. 3. Therefore, the scheme of major chronological development of the raindrop size distribution will be represented by the contours in a series in the direction shown by the open arrow. At any given time, the northern cell was more diffused than the southern ones. Combining this information with the movement of showers, the time section at any station shown in Fig. 3 will be in part the expression of changes in an order of cells I, II, and III.

6. Data selection

Values of the parameters A and b given in Table 2 show, commonly, larger differences between storms than between stations. For instance, the values of A and b determined from Station E or B and those from D or A, on the 18th, August, are rather similar in spite of the very different stage of development of the clouds as revealed in Fig. 5. It is therefore, concluded that the A and b values determined from the data from one station are significant and representative for the rain system. Thus to choose representative samples of the drop size spectrum the proximity of the $Z-R$ point to the $Z-R$ regression line will serve as an adequate criterion. The ensemble of N_D curves so selected is regarded as an expression of cloud states in different stages of development during a common weather circumstance. In Figs. 6–13 the families of the representative N_D curves are shown.

7. Basic processes for formation of a raindrop spectrum

The theory which is applied in the present paper has been discussed in the previous paper (1965*b*). There are four main processes for the development of raindrop size distributions. These are: (1) coalescence between precipitable drops, (2) mixing of raindrop groups which have individually different histories, (3) accretion of cloud droplets, involving change in concentration of the initial precipitation particles, and (4) gravitational sorting, which is a result of different fall velocities.

Process 1, coalescence between raindrops, decreases the total number of drops as rainfall intensity is increased. The raindrop size distribution resulting from this process is a monomodal spectrum. Here, the process is not affected by the way in which the initial precipitable drops are generated. If the collisions and coalescences are assumed to occur without regard to the size of the partner drops, the process is called random coalescence. The effect of this process on the size distribution is calculated in the previous paper (1961). Thus the relationship between radar reflectivity, Z, and rainfall rate, R, is given as a function of the coalescence parameters, T (m³) and N (m³) by

$$Z = 3.88 \times 10^3 \times R^{1.716}\, T^{0.716} \quad (\text{mm}^6/\text{m}^3) \qquad (3)$$

for a constant rate of collision, T. This case will be referred to as process 1*a* and in this case Z is proportional to R to the 1.7th power. For process 1*b*, an initial constant concentration of drops, N, is assumed. This yields

$$Z = 11.66 \times 10^{30} \times N^{-5} R^6. \qquad (4)$$

That is Z is proportional to R to the 6th power. Although the assumption of random coalescence seems extreme, the remarkable difference in the exponent between the processes 1*a* and 1*b*, which in initial conditions is surprising.

Process 2, mixing of raindrop groups. From past data analyses (1965*a*), it was concluded that the drop size distribution becomes a Marshall–Palmer type as the mixing takes place. The radar reflectivity Z is then proportional to R to the 1.6th power.

Process 3, accretion of cloud droplets. For accretion of cloud droplets which are not counted on the ground, two conditions are considered.

These are; $3a$ cases in which only changes in the effective thickness of cloud layer occur and $3b$ cases in which the number of precipitable particles entering the cloud layer change. On the first condition calculations with a very narrow initial size distributions show that the exponents b, is about 1.7. With broader initial spectra, b is a little larger. But in the second condition, b is approximately unity, that is, Z is proportional to R. This case produces the lowest value of b of all the processes. The process $3a$ causes the drop diameter to shift evenly to larger sizes. Therefore, the mode of the N_D curve is shifted to larger values without a remarkable decrease in the peak height.

Process 4, gravitational sorting increases the index b considerably in almost every case, sometimes up to 2.0 or even more, depending on the original size distribution and wind shear of the fall depth.

The effect of evaporation on the $Z-R$ relationships is similar to process $1b$. However, in the present analyses this will not be considered since the raindrops were sampled near cloud bases. Generally, when $b<1.7$, the value of A increases with an increasing of the mean diameter, $\bar{D}$. The radar reflectivity varies approximately as $\bar{D}^6$ and the rainfall rate, as $\bar{D}^{3.5}$. Thus from equations (1) and (2), $A = k\bar{D}^{6-3.5b}$ (5) where k is a constant.

8. Raindrop characteristics observed on the ground

(a) *Rainfall on the 31st July*

The N_D-contour section showed that the storm is much more convective at Station C than those at the two stations above. The maximum drop diameter was about 1.9 mm. The rain was very showery and the rainfall periods were very short. At station A the rain seemed more nearly continuous but exhibited some variability.

The family of N_D curves taken in the last biggest cell is shown in Fig. 6. It is more significant to note the changes in drop size distributions as the rainfall rate changes than the chronological order shown by the key. For rainfall rates below 1 mm/hr, the curves are monomodal and thus it is believed that the rainfall developed by process 3. At higher rates the curve becomes multi-modal. The peak concentration gradually increase with R but does not penetrate the level of 2000/m³ 0.2 mm. As indicated in Table 2, a remarkable feature of Hawaiian showers is that the coefficients A are less than 100. This indicates that the mean diameters are considerably small corresponding to the rainfall rates. The low value, about 1.3, for b implies that the process $3b$ contributes considerably to the rainfall growth.

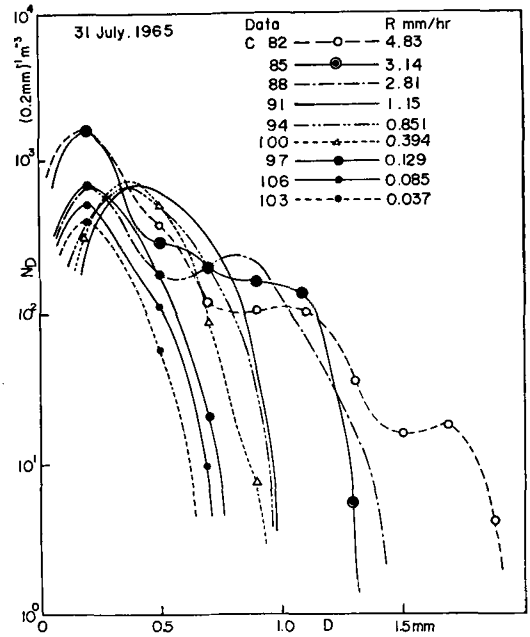

Fig. 6. Families of the representative N_D curves taken at Station C on 31st July. The way of the selection of these curves as the representative ones for the storm is presented in Section 6. The rainfall rates given in key were calculated from the raindrop data.

The curve C-100, whose rainfall rate is 0.39 mm/hr exhibits a shifted mode and has started to develop by the accretion $3a$ rather than $3b$. The curve C-88 shows that the higher rainfall rate of 2.81 mm/hr is attained by the contribution of the mixing process 2. There are two distinct groups with different modal diameters of 0.2 and 0.9 mm, showing those different growth histories in each groups.

(b) *Rainfall on the 16th August*

The N_D contour section, which is not illustrated here, indicates the pattern of moderate showers at Stations C, B and E. And the selected N_D curves are illustrated in Fig. 7.

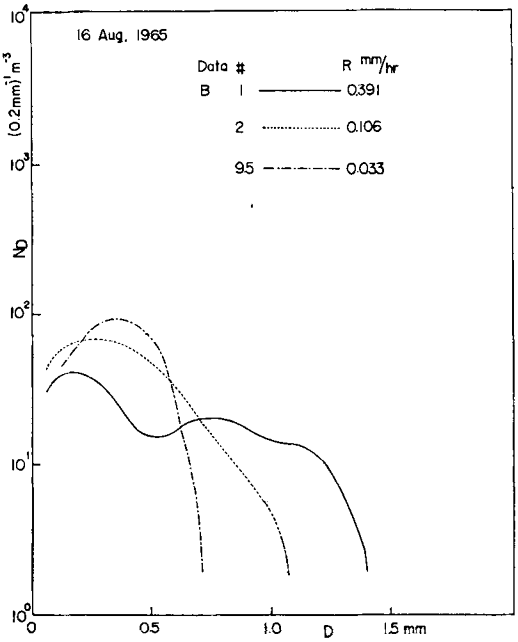

Fig. 7. Families of the representative N_D curves on 16th August. The low concentration and wide spectrum are the characteristic of this storm.

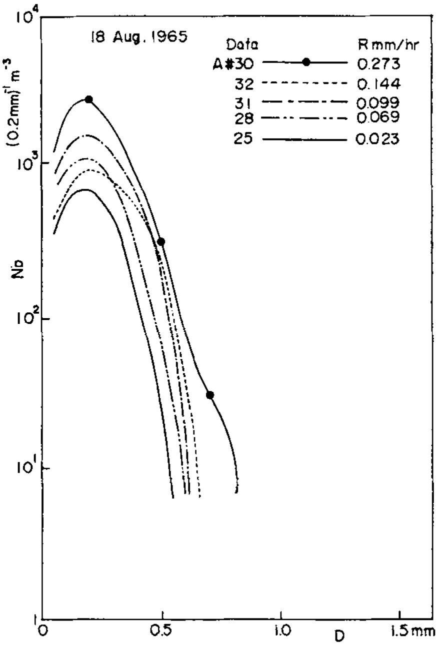

Fig. 8. Families of the representative curves on 18th August at Station A. The narrow but high peak spectrum is the characteristic of the storm of Station A.

The feature of this rain situation is that the concentrations of raindrops are rather low when rather large drops are involved, as is strikingly evident from Station B, where the value b is rather high. This feature suggests a high coalescence factor, T, which is very common in thunderstorms. Although the peak height is low, it decreases with remarkable broadening of the spectrum, implying that the major process contributing to the development is the process 1a.

(c) *Rainfall on the 18th August*

Some interpretation for this rain is given in Section 4 to 6. In Figs. 3, 8 and 9 the N_D contour sections and N_D families are illustrated, respectively. The showers were observed in a rainband as illustrated in Fig. 5. The most remarkable difference between stations is that a N_D curve taken at Station A has a high peak concentration, about 13,500 drops/mm · m³, while at other stations the corresponding peak was about 2500 drops/mm · m³. It is interesting to compare the N_D pattern with each other in Figs. 8 and 9. Although the drawing of the curve is subjective in detail, the curves at

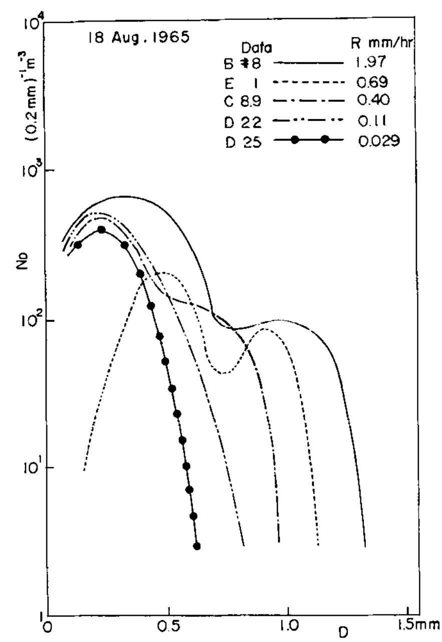

Fig. 9. Families of the representative N_D curves on 18th August. The change from one mode (D 25, and D 22) to two modes (C 8.9, E 1, and B 8) is shown.

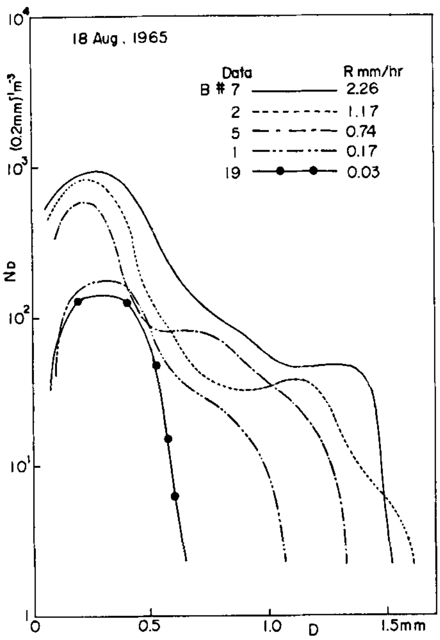

Fig. 10. Families of the representative N_D curves on 18th August at Station B. It is shown that the curve becomes skewed type with implicit multimodes.

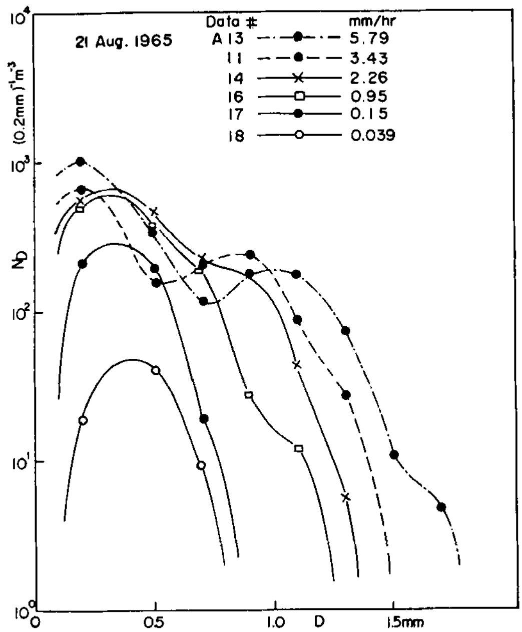

Fig. 11. Families of the representative N_D curves on 21st August at Station A. Data were taken after the rainfall maximum.

Station A are evidently monomodal. The peak heights increased with slight increase in the width. From the categories presented in Section 7, this more or less steady rain was formed by the processes 1*a* combined with 3*b*. This conclusion is based on the characteristics of N_D curves and the intermediate value of *b*. In Figs. 8 and 9, the development characteristics show that as the rainfall intensity increases process 2 becomes effective. Curve E 1 shows by the larger mode size about 0.5 mm the appreciable effect of the process 3*a* probably caused by updrafts.

(d) Rainfall on the 21st August

In Fig. 4, two remarkable convective activities are shown at Stations A and B, in front of the stratified rain. It can be seen that the concentrations of drops are relatively low. The speed of the leading edge of storm was about 700 m/min. In Figs. 11 and 12 the representative N_D families were plotted. It was noticed that the N_D curves were developed by process 1*a* combined with 3*b* until the rainfall intensity reached 0.3 mm/hr, and then mixing with larger

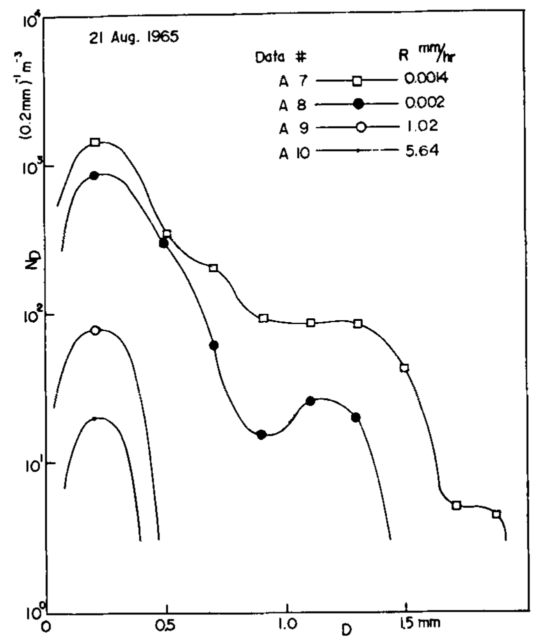

Fig. 12. Families of the representative N_D curves on 21st August at Station A. Data were taken before the rainfall maximum.

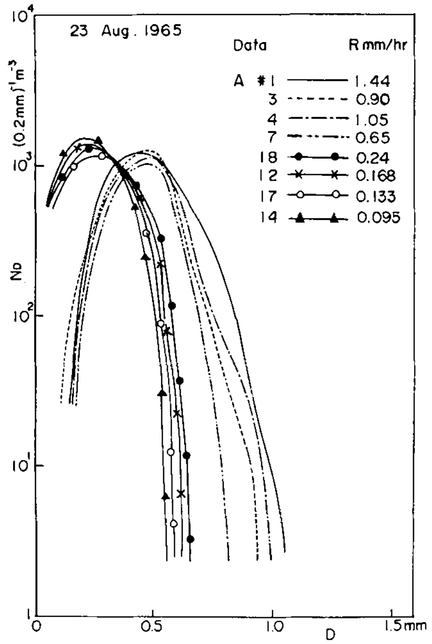

Fig. 13. Families of the representative N_D curves in the forenoon of 23rd August at Station A. The spectrum is narrow and the mean size change increases with the rainfall rate without appreciable change in the peak height.

drop groups accompanied the further increase of rainfall intensity. The families shown in Figs. 12 and 11 are the time before and the time after the mature rainfall at Station A, respectively.

It is noticed that, at the beginning of rainfall, a monomodal spectrum whose peak height is increasing is combined with a group of very large and sparsely distributed drops, whereas in the diminishing stage as shown in Fig. 11, drops are lost from larger sizes.

(e) Rainfall on the 23rd August

From the N_D contour sections it was found that, in the forenoon, the mode size of raindrops at Station A was decreasing, and the rainfall was light and continuous. The size of the largest drops was less than 1.1 mm in diameters. The two parameters A and b are less than 50 and 1.36, respectively. As shown in Fig. 13 the N_D curves show fairly constant mode height. The effective processes would be types 1b and 3a. In the afternoon, the rainfall at the mountain slope became slightly convective. The N_D patterns became to have unique variation, which imply that more seeding had occurred with an accompanying increase in the effective thickness of the cloud layer. This seems to be consistent with one of the particular models of warm rain proposed by Komabayasi (1957), because the cloud thickness and the sea salt seeding will increase when the trade wind prevails.

9. Summary

In most cases raindrop spectra develop by process 1 followed by 3 until the rainfall intensity reaches a certain value, though this critical value may change from day to day, for example it is 0.39, 0.19, and 0.34 mm/rh on the 31st July, 18th and 21st, August respectively. Further development is accompanied by the N_D curves becoming a multimodal or a widely skewed spectrum. This is result of the mixing process 2 with groups of well-developed large drops, which in turn probably develop by process 3. The primary stage consists of processes 1 and 3 and appears alone in the case of weakened convection and stratified clouds. The process 4 was hardly effective because the height of cloud base was low.

10. Analyses of b value

In Fig. 14, the vertical axis is in log Z and horizontal, in log R. Two of the regression lines for the 18th and 23rd, August, are shown on the $Z-R$ diagram (Fujiwara, 1961). In this diagram the steepest lines are for N = constant and the moderately steep lines are for T = constant, where N and T are the parameters of the random coalescence process. Accretion of cloud water with constant seeding concentration is shown by N(acc) = constant. The dotted lines with a slope 1.0 are lines of constant drop diameters. The three processes, constant coalescence 1a, constant seeding concentration 3b, and mixing 2 have the same slope of 1.6–1.7.

Consider the two points P' and Q' on the figure. These points represent a $Z-R$ relationship for the process 3b of accretion with changing numbers of initial seeds. This process corresponds well to the hypothesis that the salt nuclei concentration along with favorable accretion conditions are responsible for the rain. Now if this rain is considered to undergo further transformation by accretion or by coalecence,

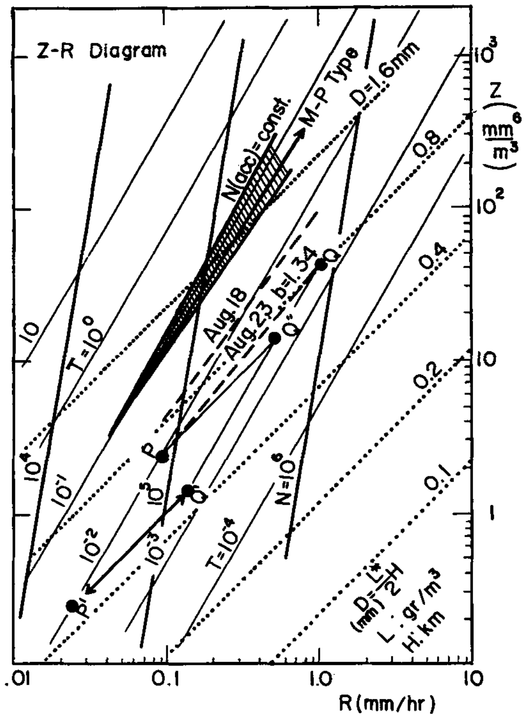

Fig. 14. Z–R diagram which interprets the processes for the rainfall development.

the points move from P' to P and Q' to Q''. The selective growth at higher rates of Q'' to Q is considered to be by coalescence. The points P and Q represent the August 23 case which was from a stratified orographic warm rain.

Process 3*b* is the only mechanism found which produces values of the slope as low as 1.1 to 1.2 which are very common in Hawaiian rains (see Table 2).

11. Conclusion

The results are compatible with the salt nuclei theory in the sense that the first stage of rain growth appears to be process 3*b* for low rainfall rates. This is clearly revealed by the examples of orographic or stratified weak rains. The process 3 is an effective one in such rains; the effect of the change in N is also evident. Although, the present analyses are not able to examine the way of growth of the initial rain drops from cloud droplets, the coalescence growth between precipitable drops, is very evident.

In Hawaiian rainshowers as shown in Fig. 2, the value b increases with A in the low b region whereas the upper part of the rainshower region shows the opposite tendency. Since the value A is responsive to the mean drop diameters, the former tendency suggest that the effect of salt nuclei on the rainfall intensity through process 3*b* gradually diminishes as convective activity is intensified. The latter tendency, though a looser correlation which was found in more or less continental data, is consistent if the raindrops are considered to have grown more through an ice-phase nuclei seeding process with more convective activity, where the seeding will effect as the process 3*b*. More intense convection will cause to activate more ice nuclei because moisture will be transported to lower temperatures.

Acknowledgements

The author wishes to express his hearty thanks to all staff scientists and cooperating members of the project for their warm and kind help through operation, discussion and data exchange. Expecially to Dr. E. A. Mueller and Prof. R. L. Lavoie for their help in writing this paper in English and for their helpful suggestions. The author is also appreciative of the encouragement and guidance for this project given to him by Dr. K. Isono. For data reduction and drawing, the author expresses his thanks to Mrs. T. Yanase and T. Koyama.

REFERENCES

Battan, L. 1956. *Radar meteorology*. University of Chicago Press.

Blanchard, D. C. 1953. Raindrop size distribution in Hawaiian rains. *Jour. Meteor. 10*, 457–473.

Blanchard, D. C. & Spencer, A. T. 1957. Raindrop measurement during Project Shower. *Tellus 9*, 541–552.

Fujiwara, M. 1965*a*. Raindrop-size distribution from individual storms. *Jour. Atmos. Sci. 22*, 585–591.

Fujiwara, M. 1965*b*. A proposed formula of raindrop size distribution *Proc. International Conf. on Cloud Phys*, pp. 265–270. Tokyo and Sapporo.

Fujiwara, M. 1961. *Raindrop size distributions with* *rainfall types and weather conditions.* Res. Rep. No. 8, III. State Water Survey, Contract No. DA-36-039 SC-87280.

Fujiwara, M. 1967. An improved raindrop radiosonde with filter paper. *Tellus, 19,* 403–407.

Komabayashi, M. 1957. Some aspect of rain formation in warm cloud (1), salinity of individual raindrops and other quantities concerning rainfall. *Jour. Met. Soc. Japan 35,* 205–220.

Rogers, R. R. & Jiusto, J. E. 1966. *An investigation of rain on the island of Hawaii,* 117 pp. Tech. Rep. CAL No. Vc-2049-p-1. Cornell Aeronautical Lab. Inc., Corn. Univ., N. Y., U.S.A.

Squires, P. & Warner, J. 1957. Some measurements in the orographic cloud of the Island of Hawaii and in trade wind cumuli. *Tellus 10,,* 475–494.

Woodcock, A. H. & Blanchard, D. C. 1955. Test of the salt-nuclei hypothesis of rain formation. *Tellus 7,* 435–448.

РАСПРЕДЕЛЕНИЕ ПО РАЗМЕРАМ КАПЕЛИ В ТЕПЛОМ ДОЖДЕ НАД ОСТ. ГАВАЙИ

Распределения дождевых капель по размерам определялись одновременно на 5 станциях на восточном склоне ост Гавайи. Из анализа этих данных было установлено, что каждая последовательность данных, полученных на одной станции, представляет собой распределение капель на различных стадиях их развития. Затем репрезентативные данные анализировались в свете предыдущей статьи автора (1965b), которая содержит классификацию 4 процесса: 1) столкновение между собой капель осадков, 2) смешение различных групп, 3) аккреция облачной воды и 4) сортировка капели.

Результаты показывают, что в большинстве случаев в течение выполнения проекта наблюдались малые величины A и b, где эти параметры определяются уравнением для радиолокационной отражаемости:

$$Z = AR^b, \quad R = \text{интенсивность дождя.}$$

Это указывает на то, что средние диаметры капель меньше, но что их число больше, чем в проливных дождях над континентами. В этом анализе подразумевается, что начальная концентрация выпадающих капелей очень эффективна в определении интенсивности дождя, особенно для орографических дождей.